33rd Annual International Conference of the IEEE EMBS
Boston, Massachusetts USA, August 30 - September 3, 2011

Optimal Trajectory Planning for a Constrained Functional Electrical Stimulation-based Human Walking

Nitin Sharma, *Member, IEEE* and Richard Stein*

Abstract

In contrast to the muscle recruitment during voluntary walking, only a limited number of muscles are activated during functional electrical stimulation (FES)-based walking. This implies that a trajectory designed or recorded from the normal human walking data may not be the best choice for tracking control. Another major challenge during FES-based walking is the rapid onset of muscle fatigue. Two methods to reduce fatigue during FES-based walking are employing an orthosis and minimizing muscle activations. To deal with these aforementioned challenges, this paper presents firstly a dynamic model representing FES-elicited walking constrained by an orthosis and a walker. Secondly, this paper deals with the design of optimal stimulation and force profiles (instead of gait-trajectories from able-bodied humans) that minimize muscle activations via FES and arm reaction forces from the walker. Ten walking steps are simulated to show the feasibility of the walking model and optimization algorithm.

1. Introduction

Functional electrical stimulation can be applied via surface, percutaneous or fully implanted electrodes to the lower extremity muscles/peroneal nerve to produce muscle contractions (i.e., hip/knee flexion and extension) that restore standing/walking in persons with gait disorders [1–6]. FES-based walking not only improves the quality of life of persons with paraplegia but is also associated with therapeutic benefits (e.g., increased muscle strength, reduction in muscle spasticity etc.) [7]. Although FES seems a promising technology many fundamental challenges need to be tackled before it gains acceptance as a regular rehabilitation technology. One crucial technical challenge is rapid onset of muscle fatigue.

Among the very few methods to deal with muscle fatigue during FES-based walking rehabilitation are: 1) utilization of an orthosis that can support body weight during standing/walking and 2) reducing intensity and duration of FES as excessive stimulation leads to rapid onset of muscle fatigue. Various prototypes of orthoses have been developed and combined with FES (see [2, 4, 5] and references therein) such as reciprocal gait orthosis (RGO) [8], controlled-brake orthosis [2], hybrid neuroprosthesis [4], joint couple orthosis [5], to name but a few. An advantage of an orthosis is that it drastically reduces the physiological effort required from the user's upper body by restraining the knees to avoid collapse during standing and stance phase of walking and also provides kinematic constraints. This also prevents continuous stimulation of quadriceps during standing and stance phase of walking as the weight of the body is supported by the orthosis, thus, reducing metabolic energy expenditure in the upper body and avoiding fatigue in quadriceps muscle due to FES.

FES is primarily used to excite lower extremity muscles or peroneal nerve during the swing phase of walking. Forward propulsion is obtained from the arm reaction forces generated by the user's arm acting on the walker. To reduce fatigue during this walking phase optimal stimulation and force profiles can be designed that minimize FES and arm reaction from the walker. This problem has been addressed to some extent in [3, 9, 10] but the main issue with these techniques is that they employ or design normal walking trajectories (representative of able-bodied persons) as a reference signal to elicit movements via FES. However, in [6] the optimal trajectories are designed using walking data from persons with paraplegia but the focus was only to minimize hand reaction force not the FES. Walking trajectories in able-bodied humans are generated through the activation of healthy muscles which in the case of persons with mobility disorders may have been atrophied or possess limited strength. Also, FES can only activate a limited number of muscles; normal walking voluntarily recruits more muscles. Due to these aforementioned reasons, tracking a normal walking gait may not be feasible or can be energetically costly in rehabilitation of walking. Therefore, new walking trajectories

*Nitin Sharma and Richard Stein are with the Department of Physiology, University of Alberta, Edmonton ALB T6G2E1 Canada. Email:{nitin.sharma, richard.stein}@ualberta.ca

that minimize fatigue due to FES and metabolic energy consumption need to be developed.

The objective of this paper is to design new optimal walking trajectories (without utilizing normal gait data) that reduce muscle fatigue and minimize metabolic energy consumption during FES-based walking. Towards this end, a human walking model that accounts for a limited number of muscle activations via FES, a knee ankle foot orthosis (KAFO) system, and a walker is developed. The model incorporates the locking and unlocking features of a modified KAFO system called Sensor Walk, manufactured by Otto Bock Minneapolis, USA. The KAFO system locks the knee joint during the stance phase to support the user's weight and unlocks the knee joint during the swing phase of the walking. Features like preventing hip flexion during the swing phase and unlocking during stance-to-swing transition phase, even when the brace is bearing user's weight, provide stability and reduced load on the user's arm muscles. The locking and unlocking of the brace on each leg is independent and is controlled through switches in the user's hands. This avoids a stiff-leg gait as observed in a RGO. The model also includes muscle dynamics required to simulate hip and knee torques evoked through FES during the swing phase. Optimization toolbox-fmincon in MATLAB was utilized to solve constrained nonlinear minimization problem and thus, find optimal stimulation and force profiles to produce walking. Algebraic impact equations were also derived to obtain a transition rule for succeeding steps. In total ten walking steps were simulated to show the feasibility of the developed model and the optimization method.

2. Three-link brace walking and impact model

In this section, a dynamic walking model is developed to represent walking using a KAFO, FES, and a walker. For model development the following assumptions and properties of the components in the FES-based walking system were used. The trunk of the user was stabilized by the walker and its dynamics was neglected in the model. The required propulsion to step forward is obtained by the user by pulling against the walker and this reaction force acts at the hip of the user. The upper body (i.e., head, arm and trunk (HAT)) is considered as a point mass. The model walks on point feet as the KAFO provides a rigid link at the foot which allows limited rotation around the ankle joint. The KAFO provides kinematic constraints as well as bears user's weight during standing and walking. The walking movement is considered only in the sagittal plane. Also, the KAFO system locks the knee joint just before the stance phase (i.e., when the swing leg is about to hit the ground) and remains locked during the stance phase. The knee joint is unlocked during the swing phase of the walking. Each leg has its own KAFO and the two braces work independently. The hip and knee muscles can be stimulated using electrodes (surface or percutaneous) to produce hip/knee flexion and extension.

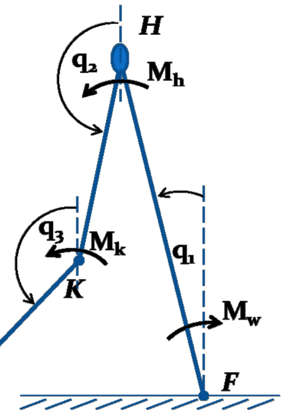

Figure 1. A three-link model representing walking with brace and the walker.

2.1. Stance and swing phase

Since the brace locks the knee joint during the stance phase, the stance leg is considered as a single segment rotating about a fixed point F on the floor as shown in Fig. 1. The swing phase generated through FES is considered as a two link segment with joints at knee (point K) and hip (Point H). The angle which the leg in stance phase makes with the vertical is denoted as $q_1 \in \mathbb{R}$ as shown in the Fig. 1. The thigh angle and the shank angle of the leg in the swing phase are denoted as $q_2 \in \mathbb{R}$ and $q_3 \in \mathbb{R}$, respectively (see Fig. 1). A Newton-Euler approach is used to derive the following dynamic equation:

$$I\ddot{\Theta} = C + G + T, \tag{1}$$

where $I \in \mathbb{R}^{3\times3}$ is the inertia matrix and $\ddot{\Theta}$ contains angular accelerations of stance segment (locked thigh and shank segment), thigh segment, and shank segment, respectively, $C \in \mathbb{R}^3$ contains coriolis terms, $G \in \mathbb{R}^3$ contains gravitational components. The elements in I, G, C are defined in the Appendix. In (1), $T \in \mathbb{R}^3$ is a joint torque vector defined as

$$T = \begin{bmatrix} M_w + M_h & M_h - M_k & M_k \end{bmatrix}^T, \tag{2}$$

where $M_w \in \mathbb{R}$ is a moment generated by the arm reaction force F_w about the fixed point F and is defined as

$$M_w = F_w l,$$

where l is the total length of the locked segment. In (2), M_h and $M_k \in \mathbb{R}$ are the torques acting at the hip joint and knee joint, respectively and are modeled as [3]

$$\begin{aligned} M_h &= M_{hf} - M_{he} - M_{hr}, \\ M_k &= M_{ke} - M_{kf} - M_{kr}, \end{aligned}$$

where $M_{hf}, M_{he} \in \mathbb{R}$ are the active hip flexion and hip extension torques, respectively, $M_{kf}, M_{ke} \in \mathbb{R}$ are the active knee flexion and knee extension torques, respectively, and $M_{hr}, M_{kr} \in \mathbb{R}$ are passive resistive torques acting at hip and knee joints, respectively. These torques are defined as

$$\begin{aligned} M_i &= \Omega_i(q_2)\Psi_i(\dot{q}_2)a_i, && \text{for } i = he, hf, \\ M_j &= \Omega_j(q_2,q_3)\Psi_j(\dot{q}_2,\dot{q}_3)a_j, && \text{for } j = ke, kf, \\ M_{hr} &= \Gamma_{hr}(q_2,\dot{q}_2), \\ M_{kr} &= \Gamma_{kr}(q_2,q_3,\dot{q}_2,\dot{q}_3), \end{aligned}$$

where $\Omega_{i,j}(\cdot), \Psi_{i,j}(\cdot) \in \mathbb{R}$ are torque equivalents of muscle force-length and muscle force-velocity relationships, respectively, and $a_{i,j} \in \mathbb{R}$ are first order muscle activation dynamics of hip flexors/extensors and knee flexors/extensors modeled as

$$\dot{a}_k = \begin{cases} (u_k - a_k)(\tau_1 u_k + \tau_2(1-u_k)), & u_k \geq a_k \\ (u_k - a_k)\tau_2, & u_k < a_k \end{cases}, \tag{3}$$

for $k = hf, he, kf, ke$ where the parameters $\tau_1, \tau_2 \in \mathbb{R}^+$ are time constants for activation and deactivation, respectively. Normalized stimulation level $u_k \in \mathbb{R}$ in (3) are modeled by the following piecewise linear curve:

$$u_k = \begin{cases} 0 & PW < thresh \\ \frac{PW-thresh}{sat-thresh} & PW >= thresh \text{ and } PW <= sat \\ 1 & PW > sat, \end{cases}$$

where $PW \in \mathbb{R}$ is the stimulation intensity (e.g., pulsewidth modulation) applied to the muscle, $thresh \in \mathbb{R}$ is the stimulation threshold level, and $sat \in \mathbb{R}$ is stimulation saturation level. See [3] for explicit definitions of aforementioned terms and muscle activation variables.

2.2. Impact phase

The leg in stance phase remains locked till the leg in swing phase impacts with the ground which also locks just before the impact occurs. This locking feature of the brace allows the three-link model to be considered as a two-link model just before and after the impact. This assumption also allows a simplified transition rule for the succeeding steps. In Fig. 2, the stance angle before and after the heel strike is denoted as q_1^- and q_1^+, respectively and similarly, the swing angle before and after the heel strike is denoted as q_2^- and q_2^+, respectively. With the assumption that the angular momentum about the impact point is conserved [11]), the following algebraic equation can be derived:

$$Q^+ = A^{-1}BQ^-, \tag{4}$$

where $Q^+, Q^- \in \mathbb{R}^4$ are the vectors containing angular position and velocity of the legs before and after the heel strike, respectively and are defined as $Q^+ = [\ q_1^+ \ \ q_2^+ \ \ \dot{q}_1{}^+ \ \ \dot{q}_2{}^+\ ]^T$, $Q^- = [\ q_1^- \ \ q_2^- \ \ \dot{q}_1{}^- \ \ \dot{q}_2{}^-\ ]^T$. The matrices $A, B \in \mathbb{R}^{4\times4}$ in (4) are defined in the Appendix.

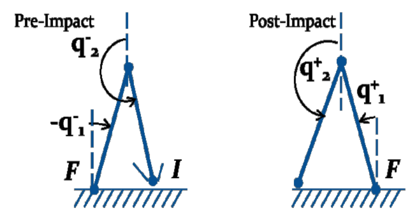

Figure 2. Just before and after the impact, the three-link model is reduced to a two-link model as in both conditions the brace locks the knee. After the impact, point *I* in the left figure becomes the fixed point *F* in the right figure (i.e., rotation point of the leg in stance phase).

3. Optimization results

In this section, the objective is to find the trajectories that minimize a function that contains cost on muscle activations of hip/knee flexor and extensors, arm reaction force from the walker, and a penalty cost on the swing leg if it tries to go below the ground level. The goal of the optimization problem is to minimize objective function $\Pi \in \mathbb{R}$

$$\Pi = \int_{t_0}^{t_f} d_1 F_w^2 + d_2 a_{h_f}^2 + d_3 a_{h_e}^2 + d_4 a_{k_f}^2 + d_5 a_{k_e}^2 + d_6 P$$

where a_k are the muscle activation dynamics of hip flexors, hip extensors, knee flexors, knee extensors defined in (3), F_w is the arm reaction force, and $P \in \mathbb{R}^+$ is a penalty for the swinging leg if it tries to go below the ground; d_i for ($i = 1$ to 6)$\in \mathbb{R}^+$ are the constant coefficients. The optimization is subject to the following constraints

$$[\ q_1(t_0) \quad q_2(t_0)\ ]^T = \alpha_1, \quad [\ q_1(t_f) \quad q_2(t_f)\ ]^T = \alpha_2,$$

$$\beta_1 < [\ \dot{q}_1(t_f) \quad \dot{q}_2(t_f)\ ]^T < \beta_2, \quad 0 < t_f < \delta,$$

$$y > 0, \quad \gamma_1 < [\ F_w \quad M_h \quad M_k\ ]^T < \gamma_2,$$

$$\varepsilon_1 < [\ q_1 \quad q_2 \quad q_3 \quad \dot{q}_1 \quad \dot{q}_2 \quad \dot{q}_3\ ]^T < \varepsilon_2,$$

where $y \in \mathbb{R}$ is the position of the hip joint relative to the ground, t_0 is the initial time of the step, t_f is the time taken to complete one step, $\alpha_1,\ \alpha_2,\ \beta_1,\ \beta_2 \in \mathbb{R}^2$, $\gamma_1,\ \gamma_2 \in \mathbb{R}^3$, $\varepsilon_1,\ \varepsilon_2 \in \mathbb{R}^4$ are known constant vectors, and $\delta \in \mathbb{R}^+$ is a known constant. Optimization for ten steps was performed by utilizing fmincon toolbox in MATLAB. For the first step, the initial angular velocities (i.e., $\dot{q}_1, \dot{q}_2, \dot{q}_3$) were zero. For succeeding steps after the first step, the initial angular velocities were computed using equation in (4). α_1, α_2 were chosen as $[\pi/9,\ \pi - \pi/9]^T$ and $[-\pi/9,\ \pi + \pi/9]^T$, respectively and for intermediate steps β_1 and β_2 were chosen as $[-\infty, -1]^T$, $[0, -0.15]^T$, respectively. Stimulation and force profile in each step were divided into six grid points where the profiles were linearly interpolated between the grid points. The computed trajectories and their corresponding stimulation and force profiles are shown in the Figs. 3 and 4, respectively.

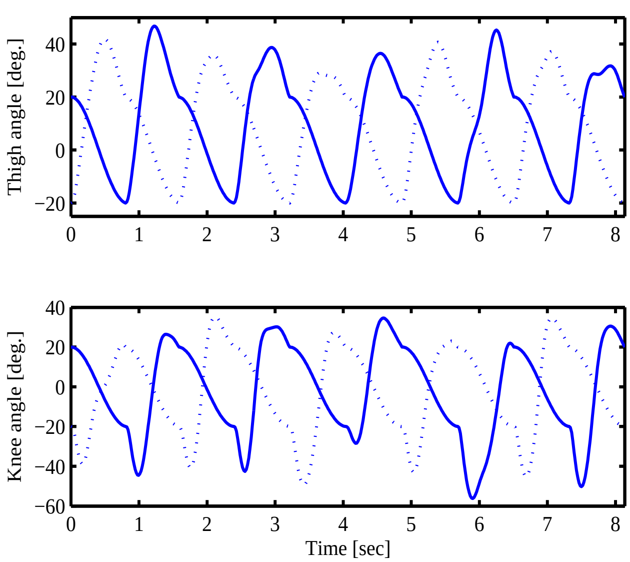

Figure 3. Trajectories depicting thigh angle ($q_2 - \pi$) and knee angle ($q_3 - \pi$) of leg 1 (starting as a stance leg, in solid line) and leg 2 (starting as a swing leg, in dotted line) over ten steps.

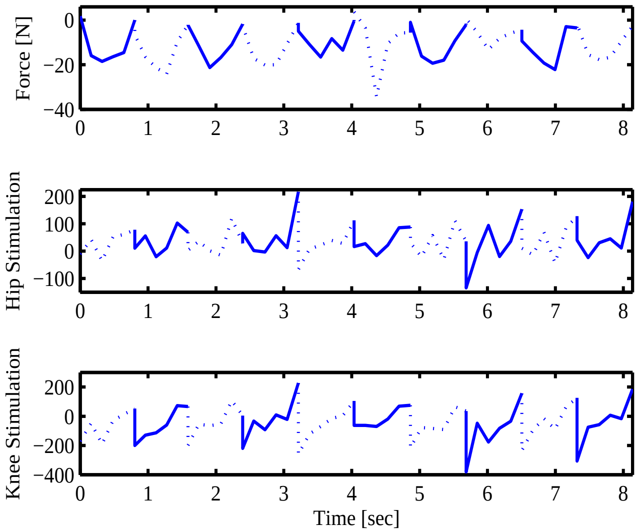

Figure 4. Optimal stimulation and force profiles of leg 1 (solid line) and leg 2 (dotted line) over tens steps. Discontinuities in the profiles are due to switching between the legs. Stimulation profiles that generate hip extension and knee flexion are shown in negative values.

4. Discussion and conclusion

The paper deals with planning optimal trajectories for a FES-based walking. The main motivation is to obtain trajectories that contain a limited number of muscle actuators and minimize fatigue. The trajectories do not require normal gait data. These trajectories can be used as reference trajectories for FES-based walking control or as optimal stimulation profiles that can be utilized to achieve FES-based walking. However, there are certain issues that will be the focus of future efforts. The current model does not consider trunk and foot dynamics. The optimal trajectories with foot dynamics are likely to be different from the trajectories obtained with point feet. We also assumed that a virtual arm reaction force required to move the user forward is automatically generated and is available all the time. However, in paraplegic walking with a walker the force from the walker is often bounded and unknown. In future these forces will be measured and profiled from experiments and realistic bounds and properties of the force will be utilized. Future efforts will also verify the developed model with experimental results and develop a more realistic model that include trunk and foot dynamics.

5. ACKNOWLEDGMENTS

This research was supported in part by the Canadian Institutes of Health Research and Alberta Innovates Health Solutions. We thank Dr. Vivian Mushahwar for helpful suggestions.

References

[1] A. Kralj and T. Bajd, *Functional electrical stimulation: standing and walking after spinal cord injury*. CRC, 1989.

[2] M. Goldfarb and W. Durfee, "Design of a controlled-brake orthosis for FES-aided gait," *IEEE Transactions on Rehabilitation Engineering*, vol. 4, no. 1, pp. 13–24, 1996.

[3] D. Popović, R. Stein, N. Oguztoreli, M. Lebiedowska, and S. Jonic, "Optimal control of walking with functional electrical stimulation: A computer simulation study," *IEEE Transactions on Rehabilitation Engineering*, vol. 7, no. 1, pp. 69–79, 1999.

[4] R. Kobetic, C. To, J. Schnellenberger, M. Audu, T. Bulea, R. Gaudio, G. Pinault, S. Tashman, and R. Triolo, "Development of hybrid orthosis for standing, walking, and stair climbing after spinal cord injury," *Journal of Rehabilitation Research and Development*, vol. 46, no. 3, pp. 447–462, 2009.

[5] R. Farris, H. Quintero, T. Withrow, and M. Goldfarb, "Design and simulation of a joint-coupled orthosis for regulating FES-aided gait," in *IEEE International Conference on Robotics and Automation*, pp. 1916–1922, IEEE, 2009.

[6] V. Nekoukar and A. Erfanian, "Optimal walking trajectories estimation using wavelet neural network for fes-assisted arm-supported paraplegic walking," in *Proc. of 10th Vienna international workshop on functional electrical stimulation*, 2010.

[7] M. Granat, A. Ferguson, B. Andrews, and M. Delargy, "The role of functional electrical stimulation in the rehabilitation of patients with incomplete spinal cord injury-observed benefits during gait studies," *Spinal Cord*, vol. 31, no. 4, pp. 207–215, 1993.

[8] M. Solomonow, R. Baratta, H. Shoji, M. Ichie, S. Hwang, N. Rightor, W. Walker, R. Douglas, and R. D'Ambrosia, "FES powered locomotion of paraplegics fitted with the LSU reciprocating gait orthoses (RGO)," in *Proceedings of the Annual International Conference of the IEEE Engineering in Medicine and Biology Society*, pp. 1672–vol, IEEE, 1988.

[9] D. Popović, M. Oğuztöreli, and R. B. Stein, "Optimal control for an above-knee prosthesis with two degrees of freedom," *Journal of biomechanics*, vol. 28, no. 1, pp. 89–98, 1995.

[10] S. Došen and D. Popovic, "Accelerometers and force sensing resistors for optimal control of walking of a hemiplegic," *IEEE Transactions on Biomedical Engineering*, vol. 55, no. 8, pp. 1973–1984, 2008.

[11] M. Garcia, A. Chatterjee, A. Ruina, and M. Coleman, "The simplest walking model: Stability, complexity, and scaling," *Journal of Biomechanical Engineering*, vol. 120, p. 281, 1998.

I, C, G, T in (1) are defined as

$$\ddot{\Theta} = \begin{bmatrix} \ddot{q}_1 & \ddot{q}_2 & \ddot{q}_3 \end{bmatrix}^T,\ I = \begin{bmatrix} p_1 & p_2 & p_3 \\ p_2 & p_4 & p_5 \\ p_3 & p_5 & p_6 \end{bmatrix},$$

$$G = \begin{bmatrix} g_1 & g_2 & g_3 \end{bmatrix}^T,\ C = \begin{bmatrix} c_1 & c_2 & c_3 \end{bmatrix}^T$$

$\ddot{q}_1$, $\ddot{q}_2$, $\ddot{q}_3 \in \mathbb{R}$ are defined as the angular accelerations of stance segment (locked brace), thigh segment, and shank segment, respectively. The elements p_i, g_i, c_i for $i = 1$ to 6 in I, G, C are defined as
$p_1 = J_1 + (m_3 + m_2)l_1^2$, $p_2 = -(m_3 l_2 l_1 + m_2 l_{2c} l_1)\cos(\phi)$,
$p_3 = -m_3 l_{3c} l_1 \cos(\varphi)$, $p_4 = m_3 l_2^2 + J_2$,
$p_5 = m_3 l_{3c} l_2 \cos(\psi)$, $p_6 = J_3$,
$g_1 = (-m_1 l_{1c} - m_h l_1 - m_3 l_1 - m_2 l_1) g \sin(q_1)$,
$g_2 = m_2 g l_{2c} \sin(q_2) + m_3 g l_2 \sin(q_2)$, $g_3 = m_3 g l_{3c} \sin(q_3)$,
$c_1 = \sin(\phi)(m_3 l_2 l_1 + m_2 l_{2c} l_1)\dot{q}_2{}^2 + m_3(l_{3c} l_1 \sin(\varphi)\dot{q}_3{}^2$
$c_2 = (m_3 l_2 + m_2 l_{2c}) l_1 \dot{q}_1{}^2 \sin(\phi) - m_3 l_{3c} l_2 \sin(\psi)\dot{q}_3{}^2$,
$c_3 = m_3 l_{3c} l_1 \sin(\varphi)\dot{q}_1{}^2 + m_3 l_{3c} l_2 \sin(\psi)\dot{q}_2{}^2$,
where $\phi, \varphi, \psi \in \mathbb{R}$ are defined as $\phi = q_1 - q_2, \varphi = q_1 - q_3, \psi = q_2 - q_3$, respectively, m_2, m_3, $m_h \in \mathbb{R}$ are the mass of the thigh, shank, and HAT, respectively, $m_1 \in \mathbb{R}$ is defined as $m_1 = m_2 + m_3$, l_2, $l_3 \in \mathbb{R}$ are the lengths of the thigh and shank, respectively, $l_1 \in \mathbb{R}$ is defined as $l_1 = l_2 + l_3$. $l_{2c} \in \mathbb{R}$ is the location of center of gravity (COG) of the thigh as measured from the hip joint, $l_{3c} \in \mathbb{R}$ is the leg COG location as measured from the knee joint, $l_{1c} \in \mathbb{R}$ is defined as $l_{1c} = (m_3(l_3 - l_{3c}) + m_2(l_1 - l_{2c}))/m$; J_2, $J_3 \in \mathbb{R}$ are the thigh inertia and the shank inertia about hip joint, respectively, $J_1 \in \mathbb{R}$ is the shank inertia about the contact point on the ground. The matrices A and B in (3) are defined as

$$B = \begin{bmatrix} -1 & 0 & 0 & 0 \\ 2 & 1 & 0 & 0 \\ 0 & 0 & \begin{matrix} -2m_1 l_1 l_{1c}\cos(\phi^-) - \\ m_1 l_{1c} l_{2c} - m_h l_1^2 \cos(\phi^-) \end{matrix} & -m_1 l_{1c} l_{2c} \\ 0 & 0 & -l_{2c} l_{1c} & 0 \end{bmatrix},$$

$$A = \begin{bmatrix} 1 & 0 & 0 & 0 \\ 0 & 1 & 0 & 0 \\ 0 & 0 & \begin{matrix} m_l l_{1c}^2 + m_h l_1^2 + m_1 l_1^2 + \\ m_1 l_{2c} l_1 \cos(\omega^-) \end{matrix} & \begin{matrix} m_1 l_{2c}^2 + \\ m_1 l_{2c} l_1 \cos(\omega^-) \end{matrix} \\ 0 & 0 & l_{2c} l_1 \cos(\omega^-) & l_{2c}^2 \end{bmatrix},$$

where $\phi^- = q_1^- - q_2^-$ and $\omega^- = q_2^- + 3q_1^-$